*Anal. Chem.* **2009,** *81,* 5972–5979

analytical chemistry
feature

# Fluorescent-Protein-Based Biosensors: Modulation of Energy Transfer as a Design Principle

**Robert E. Campbell**

*University of Alberta*

**Genetically-encoded biosensors based on FRET between fluorescent proteins of different hues enable quantitative measurement of intracellular enzyme activities and small molecule concentrations. (To listen to a podcast about this feature, please go to the *Analytical Chemistry* website at pubs.acs.org/journal/ancham.)**

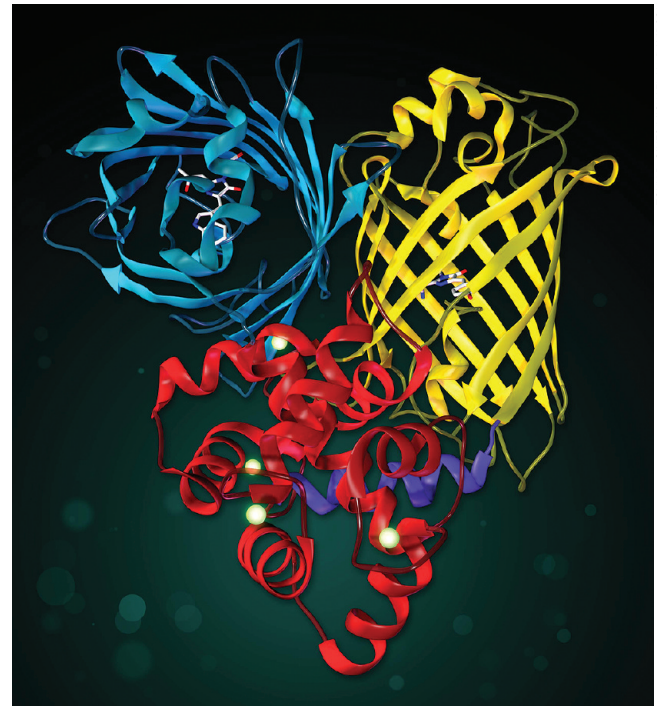

TONY B. GINES/MICHAEL W. DAVIDSON

The definition of a "biosensor"—that is, a detection system that relies on a biomolecule for molecular recognition and a transducer to produce an observable output[1]—is firmly established in the lexicon of analytical chemistry. However, in recent years, biochemists appropriated the term biosensor to refer to genetically-encoded, designed proteins that are self-sufficient detection systems for a variety of targets, including small molecules and enzymes. The molecular recognition component of a biosensor is a protein, and this is also true for genetically-encoded biosensors. The primary difference between conventional biosensors and genetically-encoded biosensors is the nature of the transducer. Traditionally, the transducer is any one of a wide assortment of synthetic and modified surfaces that are electrochemically or optically sensitive to the action of the biomolecule. In contrast, the choice of transducer for a soluble and discrete genetically-encoded biosensor is constrained to being genetically encoded. Fortunately, one particular transducer format has proven to be exceptionally versatile for the construction of these biosensors: the modulation of Förster (or fluorescence) resonance energy transfer (FRET) between genetically fused fluorescent proteins (FP) of differing hues.[2]

The use of recombinant FPs for live-cell fluorescence imaging made its dramatic debut in 1994, when an image of a nematode worm with a green fluorescent neuron appeared on the cover of *Science*.[3] Ever since, the popularity and number of applications of FPs have increased at a dramatic pace. The single overwhelming advantage of FPs as fluorophores for live-cell applications is that, unlike synthetic dyes or quantum dots, they do not need to be manually introduced into the cell. A cell or organism containing an appropriate FP transgene can synthesize the FP polypeptide using intrinsic cellular transcriptional and translational machinery.[3] The nascent FP polypeptide then folds and autonomously undergoes posttranslational modifications to form a visible wavelength fluorophore buried deep within its $\beta$-barrel structure.[4] Through the efforts of protein engineers, a complete spectrum of FP variants—ranging from blue to far red[5]—are now available, all of which are close structural homologues of the archetypical *Aequorea* green FP (GFP).

The most common applications of FPs do not involve genetically-encoded biosensors but rather use FPs as reporters of gene expression or as markers for the localization of specific organelles or recombinant fusion proteins in live cells.[6,4] Design and construction of gene chimeras for these applications are relatively simple, and considerations are generally limited to the relative merits of N- versus C-terminal fusions and the length of flexible



10.1021/ac802613w CCC: $40.75 
Published on Web 06/24/2009

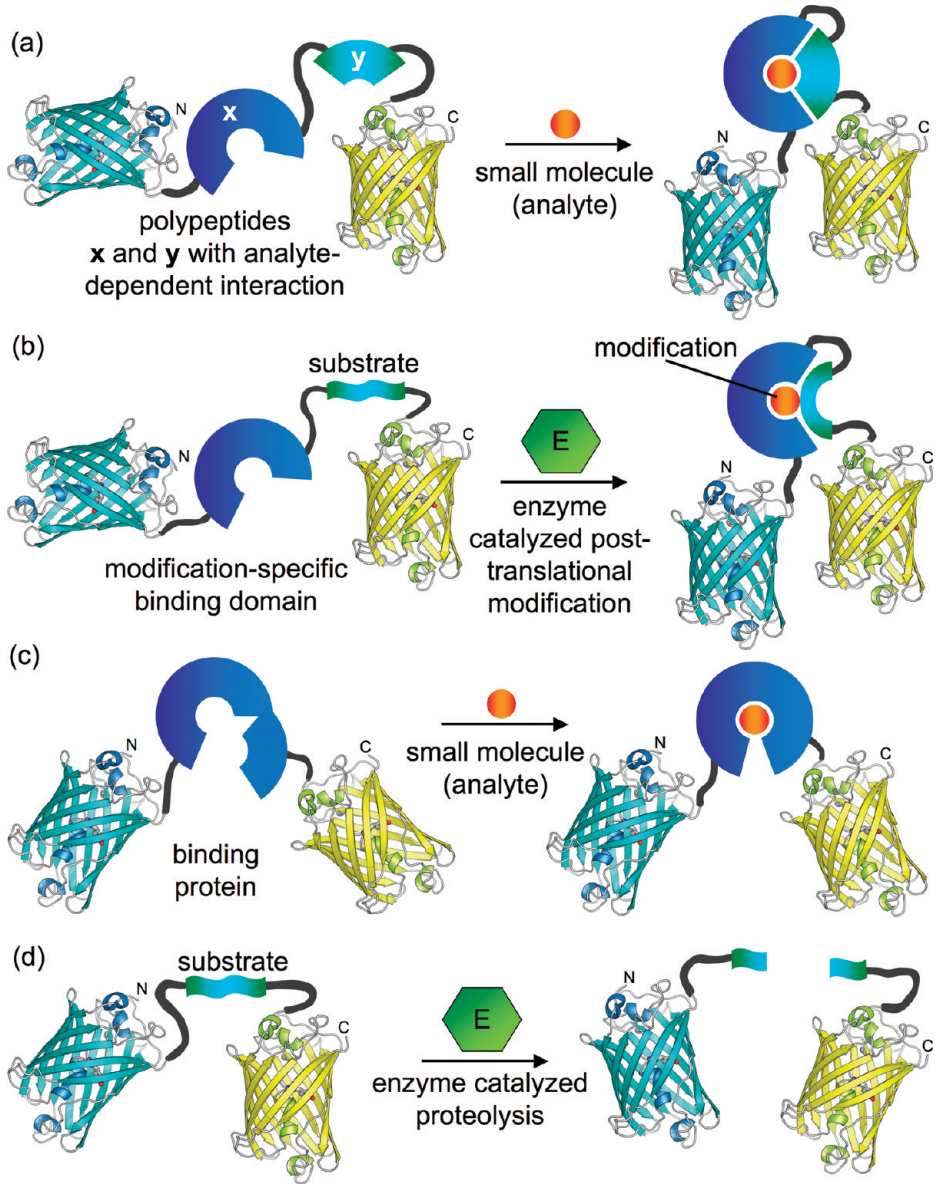


**Figure 1.** Representative FRET-based biosensors for enzyme activities and small molecule analytes. Although the donor is cyan and the acceptor is yellow in these representations, a variety of other hues could be substituted. (a) Biosensors in which binding of a small molecule induces the association of two distinct moieties within the polypeptide chain.[2] (b) Biosensors for posttranslational modification.[48,49] (c) Biosensors in which a single binding protein undergoes a conformational change upon binding its small molecule ligand.[33] (d) Biosensors for protease activity.[50]

linker to be incorporated.[7] Researchers interested in imaging multiple proteins simultaneously in a live cell can choose from a broad selection of spectrally distinct hues. For example, using a widefield fluorescence microscope with appropriate filter sets, cyan (CFP), yellow (YFP), orange (OFP), and red (RFP) FPs can be imaged in the same cell with acceptably low amounts of undesirable fluorescent signal bleed through between emission channels.[8] The use of spectral imaging with linear unmixing has enabled as many as six distinct hues to be resolved using only a single laser line for excitation.[9]

In terms of number of published reports, applications of genetically-encoded biosensors are dwarfed by the applications described in the preceding paragraph. One of the primary reasons for this discrepancy is that FP-based biosensors are non-trivial to design, construct, optimize, and use. These perceived challenges have likely limited the number of research groups willing to invest the resources necessary to bring the development of a new FP-based biosensor to fruition. In this article, I will argue that the actual challenges are not as great as once thought. Over the last few years, a number of groups have been working to not only create new biosensors but also to develop new strategies for their design and optimization.[10] One major lesson to be learned from these efforts is that biosensor designs based on modulation of FRET between two FPs are, generally speaking, more amenable to rational design and more broadly applicable than biosensor designs based on modulation of fluorescence from a single FP.[11,12]

This article will provide a basic theoretical framework for understanding the design and optimization of FRET-based biosensors and then use this framework as a basis for dissecting some examples. From this analysis emerges a series of guidelines that should greatly facilitate future efforts to develop new genetically-encoded biosensors.

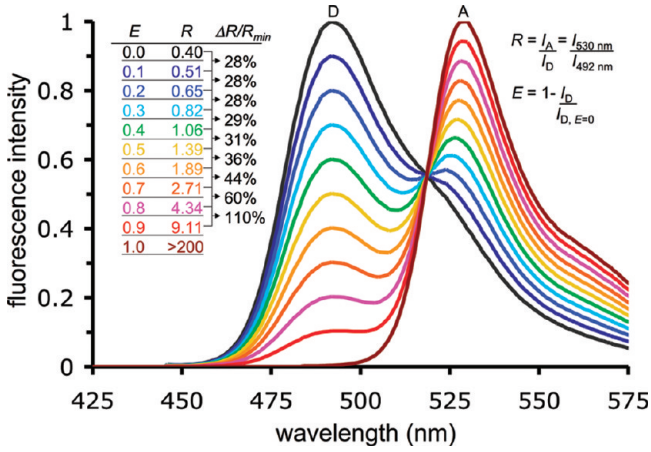


**Figure 2.** The relationship between $E$ and $R$. The $\Delta R/R_{min}$ has been calculated for each increment of $\Delta E = 0.1$. Spectra are simulated for the mTFP1/YFP FRET pair.[51]

## BASIC DESIGN

The key to designing a successful FRET-based biosensor is to identify and exploit a mechanism by which a specific binding interaction or modification of a protein or peptide can be transduced into a substantial modulation of FRET efficiency ($E$) between donor and acceptor FPs. Some of the most effective designs are represented in Figure 1. FRET is the distance- and orientation-dependent radiationless transfer of internal energy from a higher-energy donor fluorophore to a lower-energy acceptor chromophore.[13,14] A higher $E$ means that more of the donor's internal energy is being passed to the acceptor, and thus the intensity of the donor's characteristic emission profile is proportionally quenched (Figure 2). FRET does not require the acceptor to be fluorescent, but if it is, it will fluoresce with its characteristic emission profile just as though it had been excited directly.

The FRET phenomenon is highly conducive to quantitative measurement by ratiometric imaging of emission intensity or imaging of the donor fluorescence lifetime.[15] For ratiometric imaging, the biological specimen is illuminated with wavelengths of light that preferentially excite the donor FP while images of the fluorescence emission from the specimen are collected through two different emission bandpass filters corresponding to the emissions of the donor and acceptor. If the two FPs are far apart in space (> 10 nm), the efficiency of energy transfer will be negligible ($E \approx 0$), and the unquenched fluorescence of the donor will be observed. In the absence of energy transfer, some emission from the acceptor FP may occur due to direct excitation. As the two FPs are brought closer together in space, $E$ increases towards a theoretical upper limit of unity, and the intensity of the acceptor emission increases at the expense of the donor emission (Figure 2). Experimentally, this change is manifested as a decrease in the intensity measured through the donor filter ($I_D$) and an increase in the intensity measured through the acceptor filter ($I_A$). The ratio of acceptor to donor fluorescence intensity ($R = I_A/I_D$) is typically used as a surrogate for $E$ in live-cell imaging. For a FRET-based biosensor, a change in ratio ($\Delta R = R_{max} - R_{min}$) is experimentally measured, and maximizing this value is of the utmost concern when optimizing a biosensor. For the sake of consistency, ratio changes have been converted to percentage changes in the form of $\Delta R/R_{min}$.

## THE MATHEMATICS OF FRET EFFICIENCY

A simple mathematical formula describes the change in FRET efficiency ($\Delta E$) as a function of the interfluorophore distance and orientation factors in the initial and final states of the biosensor. In the initial state, the efficiency of energy transfer ($E_{initial}$) is described by

$$E_{initial} = \frac{1}{1 + \frac{r_{inital}^6}{r_{o,initial}^6}} \quad (1)$$

in which $r_{initial}$ is the interchromophore distance and $r_{o,initial}$ is the initial Förster distance.[13,14] (Although $R_o$ is most often used to represent Förster distance, I use $r$ for all distances, including the Förster distance, and $R$ for ratios.) The Förster distance is described by

$$r_{o,initial}^6 = 8.8 \times 10^{-28} \kappa_{initial}^2 n^{-4} \Phi_D J \quad (2)$$

in which $\kappa_{initial}^2$ is the orientation factor, $n$ is the refractive index, $\Phi_D$ is the quantum yield of the donor, and $J$ is the overlap integral. Of these four terms, only $\kappa^2$ could potentially differ in value between the initial and final states of the biosensor under typical imaging conditions. Accordingly, we can define constant $C$ ($8.8\times10^{-28} n^{-4} \Phi_D J$) and substitute it into the equation for $E_{initial}$:

$$E_{initial} = \frac{1}{1 + \frac{r_{initial}^6}{C\kappa_{initial}^2}} \quad (3)$$

Similarly, the final FRET efficiency ($E_{final}$) can be expressed as a function of $r_{final}$ and $\kappa_{final}^2$. Thus for a FRET-based biosensor, the $\Delta E$ from the initial to the final state is

$$\Delta E = \left| E_{final} - E_{initial} \right| = \left| \frac{1}{1 + \left( \frac{r_{final}^6}{C\kappa_{final}^2} \right)} - \frac{1}{1 + \left( \frac{r_{initial}^6}{C\kappa_{initial}^2} \right)} \right| \quad (4)$$

In this equation, four variables determine the magnitude of $\Delta E$ for a FRET-based biosensor: $r_{initial}$, $r_{final}$, $\kappa_{initial}^2$, and $\kappa_{final}^2$. To achieve a non-zero value of $\Delta E$, the specific binding interaction or modification of the FRET-based biosensor must result in either a change in interchromophore distance or a change in orientation factor between the initial and final states.

## $\Delta E$ AND $\Delta R/R_{MIN}$: HOW MUCH IS ENOUGH?

The key to creation of a successful FRET-based biosensor is that the $\Delta E$ must be large enough to provide a robust change in $\Delta R/R_{min}$ with an acceptable S/N. So how large do $\Delta E$ and the more practical value of $\Delta R/R_{min}$ need to be? The short answer is that both must be as large as possible. The long answer aims to set a lower boundary on these values that defines a minimally sufficient criterion for success. Based on literature precedent, a FRET-based biosensor that is useful in live cell imaging should have $\Delta E \geq 0.1$ and $\Delta R/R_{min} \geq 30\%$. If $\Delta E = 0.1$, then $\Delta R/R_{min}$ is ~30%, even at a relatively low absolute $E$ of 0.1−0.3

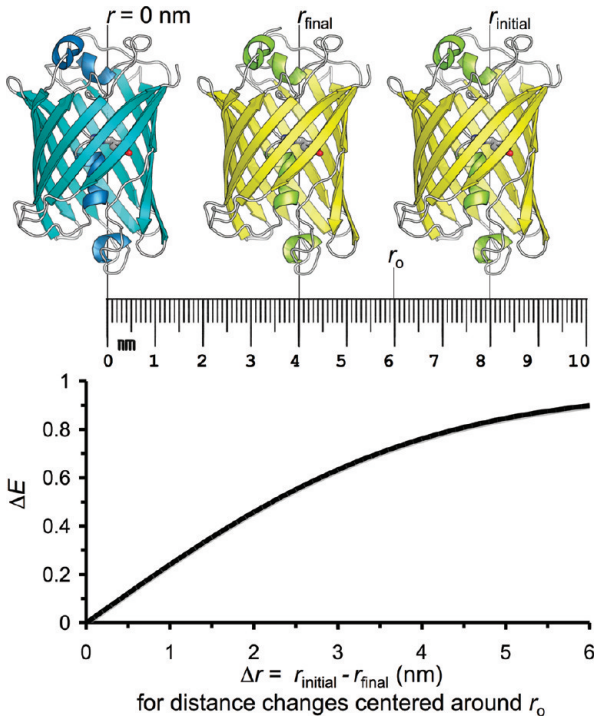


**Figure 3.** The effect of distance changes centered around $r_o$ on $\Delta E$ as calculated using Equation 4 with $\kappa^2_{initial} = \kappa^2_{final} = 2/3$. An $r_o$ value of 6 nm—i.e., the mTFP1/Venus pair[52]—is used in this representation. At the top of the figure is a to-scale representation of the acceptor (yellow) at distances of 8 nm ($r_{initial}$) and 4 nm ($r_{final}$) from the donor (teal). A biosensor in which the acceptor moves from this initial to this final distance would have a $\Delta r$ of 4 nm and a very impressive $\Delta E$ of 0.77.

(Figure 2). Because there is a nonlinear relationship between $E$ and $R$, $\Delta E = 0.1$ can result in a substantially higher $\Delta R/R_{min}$ at a high $E$.

An important caveat that accompanies the long answer is that these criteria are only applicable when the dynamic range of the biosensor matches the biologically relevant concentrations. For example, it is critical that the affinity of $Ca^{2+}$ biosensors approximates the biologically relevant range within which fluctuations in concentration are expected to occur.[2] Another caveat is that it might be possible to use biosensors with $\Delta R/R_{min} <$ 30%, provided that the expression level is high enough and/or the microscope optics and camera are of sufficient quality and efficiency to provide a satisfactory S/N. Yet another consideration is that at very high $R$, one of the two emission channels is necessarily dim and has a correspondingly lower S/N. For this reason, a $\Delta R/R_{min}$ of 100% due to a change in ratio from 1 to 2 is preferable to a $\Delta R/R_{min}$ of 100% due to a change in ratio from 5 to 10.

## $\Delta r$ AND $\Delta\kappa^2$: HOW MUCH IS ENOUGH?

How large do $\Delta r$ and $\Delta\kappa^2$ need to be to achieve the minimally sufficient $\Delta E = 0.1$? A plot of the relationship between $\Delta r$ and $\Delta E$ for changes centered at $r_o$ addresses this question (Figure 3). This graph reveals that a relatively modest $\Delta r$ of just 0.4 nm centered at $r = r_o$ (6 nm in this example) provides the minimally sufficient $\Delta E = 0.1$. $E$ is most strongly dependent on $r$ at $r = r_o$; at distances either larger or smaller than $r_o$, larger changes are required to attain similar values of $\Delta E$. For the example

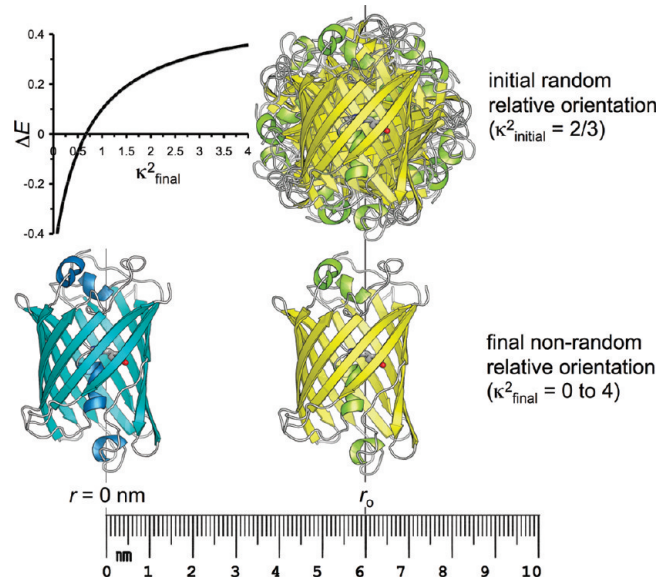


**Figure 4.** The effect of $\kappa^2$ changes on $\Delta E$ as calculated using Equation 4 with $r_{initial} = r_{final} = r_o$. Calculations assume an initially random orientation of transition dipoles ($\kappa^2_{initial} = 2/3$), as might be expected for the less compact state of biosensors of the types shown in Figure 1a–c. The value of $\kappa^2_{final}$ describes the orientation of the transition dipoles following the conformational change that occurs upon posttranslational modification or binding of analyte.

shown in Figure 3, a 1 nm $\Delta r$ from 7.5 to 8.5 nm or from 3.4 to 4.4 nm would also provide the minimally sufficient $\Delta E = 0.1$. In the case of biosensors for proteolysis (Figure 1d) or detection of intermolecular protein–protein interactions, $\Delta E > 0.1$ is readily achieved because the larger of the two distances is effectively infinite.

A discussion of the effect of changes in $\kappa^2$ on $\Delta E$ is hampered because the relationship is mathematically complex and difficult to understand at an intuitive level. Fortunately, a simplified model of $\kappa^2$ can capture its most important aspects. $E$ depends on the relative orientation of the transition dipoles of the donor and acceptor. Aligned dipoles are described with a value of $\kappa^2 = 4$ and will result in the highest possible $E$ at a given distance. Perpendicular dipoles are described with a value of $\kappa^2 = 0$ and will result in $E = 0$ at any distance. At intermediate orientation angles, $\kappa^2$ has a value of 0–4. This simple model is complicated by the fact that $E$ is an ensemble measurement and is thus averaged over many molecules that are spinning and tumbling in space and adopting countless different relative dipole orientations. Averaging of $\kappa^2$ over all possible random orientations gives $\kappa^2 = 2/3$, which is generally acceptable for calculating distances from experimental $E$ values.[16]

For FRET-based biosensors, a common practice is to include regions of unstructured polypeptide linker that will provide little, if any, restriction on the tumbling and twisting of the attached FP.[7] In these cases, the assumption of $\kappa^2 = 2/3$ is almost certainly valid. However, it is reasonable to envision scenarios in which the unstructured linker is minimized and both FPs are partially restricted in mobility such that the chromophore dipoles are biased towards either a particularly favorable ($\kappa^2 > 2/3$) or unfavorable ($\kappa^2 < 2/3$) orientation for FRET. Plotted in Figure 4 is the expected $\Delta E$ as a function of $\kappa^2$ for a biosensor that has switched from an initially random dipole orientation to a biased

dipole orientation at a constant interchromophore distance. If the transition dipoles remain randomly oriented in the final state, $\kappa^2_{final} = \kappa^2_{initial} = 2/3$ and $\Delta E = 0$. In order to achieve the minimally sufficient $\Delta E = 0.1$, a $\kappa^2_{final}$ of 1 or 0.44 is required.

This discussion has so far treated the distance- and orientation-dependence of $E$ in isolation from one another. In practice, both factors may be simultaneously contributing to the overall $\Delta E$. Assuming that the individual contributions complement each other, the actual changes in distance and orientation could each be less than the minimally sufficient changes suggested above. Ideally, a biosensor should undergo an inducible switch between one state that is less compact (higher $r$) and has random or unfavorable dipole orientations ($\kappa^2 \leq 2/3$) and a second state that is more compact (lower $r$) and has favorable dipole orientations ($\kappa^2 > 2/3$).

## DISTANCE VERSUS ORIENTATION CHANGES

Distance changes are generally more important than orientation changes for creating effective FRET-based biosensors because logic and intuition can provide the basic blueprint for successful biosensors that are based on $\Delta r$. This is particularly true when the atomic structures of the protein domains of interest can be downloaded from the Protein Data Bank archive and viewed using molecular graphics software. In contrast, the subtlety and complexity of $\kappa^2$ obfuscates the successful rational design of biosensors based primarily on orientation changes. Accordingly, researchers generally rely foremost on designed distance changes to achieve satisfactory $\Delta E$ values. Optimization of $\kappa^2$ is a secondary concern usually achieved by empirical optimization approaches such as the screening of large libraries of variants with randomized linker lengths or other substitutions. An exception to this rule is the class of biosensors represented in Figure 1c, for which $\kappa^2$ modulation may be more important than distance modulation.

The yellow cameleon (YC) class of $Ca^{2+}$ biosensors[2] is the prototypical example of a successful biosensor of the type shown in Figure 1a. YC was initially designed to operate primarily by distance modulation and has since been subjected to extensive empirical optimization.[17−19] A version of this biosensor, YC3.60, exhibits a remarkable $\Delta R/R_{min} = 560\%$.[18] A $\Delta R/R_{min}$ of this magnitude could be obtained if $E$ changed from ~0.5 to ~0.9 (Figure 2). Indeed, a detailed photophysical study of YC3.60 revealed a change in $E$ from 0.5 to >0.9.[20] The authors also examined the relative importance of distance and orientation changes and arrived at two important conclusions. First, even slight changes in conformation due to free rotations within a flexible linker could give rise to any value of $\kappa^2$ at a given fixed distance. Second, even in this highly optimized version of the biosensor, $\Delta r$ (modeled as a change from 4.9 to 2.6 nm) was primarily responsible for the modulation of $E$; $\kappa^2$ modulation was largely irrelevant.

In an effort to use computational approaches to supplement or replace the role of human intuition and logic in the design of FRET-based biosensors, Pham et al. have developed the Fusion Protein Modeler tool.[21] This software can construct models of biosensors based on published atomic coordinates and perform rigid body simulations of conformational dynamics by varying dihedral angles in flexible linker regions. Based on the positions of the donor and acceptor in this sampling of conformational space, average distances and orientation factors can be calculated for both the less compact and more compact states of a biosensor. The authors applied this analysis to a series of YC constructs and obtained reasonable qualitative agreement with experimental data. One interesting result was that for the 20 distinct predictions that were performed, average $\kappa^2 = 0.68 \pm 0.15$. This tight distribution of $\kappa^2$ centered at the value associated with random dipole orientations ($\kappa^2 = 0.67$) further illustrates the challenge of engineering a biosensor in which at least one state has an average dipole orientation with substantial bias towards a non-random orientation.

In the following sections I will examine some illustrative examples of design and optimization strategies that have proven useful in the development of new FRET-based biosensors. A clear trend that runs through all of these examples is that although logic and biochemical intuition guide the initial design of FRET-based biosensors, subsequent efforts to maximize the value of $\Delta E$ is almost always an empirical process.

## MAXIMIZING $\Delta R/R_{MIN}$: DISTANCE CHANGES

For proteolysis biosensors (Figure 1d), the strategy for maximizing the FRET change is readily apparent: the donor and acceptor should be as close as possible in the initial (intact) state of the biosensor. However, if the linkers are too short, the steric bulk of the FPs may adversely affect the accessibility of the substrate to the active site and slow the rate of the reaction. For example, to maximize the $\Delta R/R_{min}$ for a biosensor of anthrax lethal factor (LF) protease, Kimura et al. examined the effect of linker length on $\Delta R/R_{min}$ and rate of proteolysis.[22] They found that the rate increased and the $\Delta R/R_{min}$ decreased as linker length increased. To pick the "optimal" biosensor, the authors chose a construct with a smaller $\Delta R/R_{min}$ (790% versus a best of 1270%) but an increased rate of cleavage.

In contrast to the relatively subtle change in donor−acceptor distance for biosensors of the type represented in Figure 1c, a relatively large change in donor−acceptor distance is inherent in the design of biosensors of the types schematically represented in Figures 1a and 1b. However, for these biosensors, the relationship between linker length and $\Delta E$ is less obvious than the relationship for biosensors of proteolysis. Because the donor and acceptor are covalently linked in both the initial and final states, any change in linker length will affect both the initial and final distances. To maximize the FRET change, an improved linker combination should decrease $r$ in the more compact state and increase $r$ in the less compact state. To a first approximation, this selective increase in $r$ for the less compact state can be rationally achieved by lengthening the middle linker (that is, the linker between **x** and **y** in Figure 1a or between domain and substrate in Figure 1b). Changes in linker length that affect the interchromophore distance in both states by the same amount are neutral with respect to the $\Delta r$. However, a new linker combination with an equivalent $\Delta r$ can produce an improved $\Delta E$ if the mean distance is closer to $r_o$. Furthermore, even if $\Delta E$ is equivalent, an improved $\Delta R/R_{min}$ can result if the mean $E$ has increased (Figure 2).

The complex interplay between $\Delta r$, $\Delta E$, and $\Delta R/R_{min}$ means that researchers generally rely on the systematic modification of linker lengths and empirical screening to identify improved biosensors. Two recent reports of $Zn^{2+}$ biosensors illustrate

how this complexity can sometimes lead to unanticipated trends in the FRET response. The first report concerned a biosensor for $Zn^{2+}$ with hexahistidine tags fused to the N- and C-termini of the donor and acceptor.[23] Addition of $Zn^{2+}$ induces an intramolecular association of the hexahistidine tags that brings the FPs into closer proximity. Screening of linker-length variants revealed that the longest linkers produced the highest $\Delta R/R_{min}$ (60%). This result is consistent with expectations because a longer linker would be expected to increase $r$ for the less compact state and not affect $r$ for the more compact state. The $Zn^{2+}$ biosensor of the second report is schematically identical to that shown in Figure 1a; in this case, **x** and **y** are two different protein domains that undergo a $Zn^{2+}$-dependent association.[24] To optimize the response of this biosensor, the authors screened a variety of lengths of linker between **x** and **y**. Contrary to expectations, the authors found that addition of $Zn^{2+}$ caused $E$ to *decrease* for all linker lengths and the shortest linker tested had the highest $\Delta R/R_{min}$ (57%). Presumably, in the $Zn^{2+}$-bound state of the biosensor, the donor and acceptor are rigidly held at a greater average distance than in the $Zn^{2+}$-free state. This conclusion was consistent with the results of a molecular modeling study, which revealed that the greater conformational freedom in the $Zn^{2+}$-free state produced a smaller average distance between the donor and acceptor.

To maximize $\Delta r$, it is also desirable to decrease $r$ in the more compact state. Although the $\beta$-barrel shells of the FPs limit how close the fluorophores can be, researchers can minimize $r$ by using a pair of "sticky" FPs known as CyPet (donor) and YPet (acceptor).[25] This pair of engineered FPs forms a heterodimeric complex at sufficiently high effective molarity.[26,27] The close approach and possibly favored orientations of the fluorophores in the heterodimeric complex cause a very high $E$ for the compact state. By exploiting this high efficiency, researchers have developed protease biosensors (Figure 1d) with $\Delta R/R_{min}$ values of 2000%.[25] Indeed, CyPet/YPet were used to achieve the very high $\Delta R/R_{min}$ for the LF protease biosensor mentioned earlier.[22] The use of "sticky" FPs has also greatly improved $\Delta R/R_{min}$ for $Ca^{2+}$[28] and kinase[29,28] biosensors of the types shown in Figures 1a and 1b, respectively. A $Zn^{2+}$-biosensor that chelates $Zn^{2+}$ to cysteine and histidine residues on the surfaces of the FRET pair to bring them into close proximity might be said to be taking advantage of "analyte specific stickiness".[30] The extreme example of CyPet/YPet aside, color variants derived from GFP exhibit a weak tendency to dimerize unless they have been specifically engineered to be monomeric;[31] this feature is important for the FRET response of some biosensors.[32]

Lengthening of linkers that increase $r$ in the less compact state and minimizing $r$ in the more compact state through the use of dimerizing FPs illustrate two of the most effective rational strategies for maximizing $\Delta r$. However, the examples of the $Zn^{2+}$ biosensors show that pursuing rational designs without empirical screening is improvident and may prevent the discovery of unanticipated solutions.

## MAXIMIZING $\Delta R/R_{MIN}$: ORIENTATIONS

For the class of biosensors represented in Figure 1c, only a relatively subtle conformational change accompanies binding of the target analyte. Accordingly, a protein engineer cannot rely only on $\Delta r$ to achieve a minimally sufficient $\Delta E$; some degree of $\kappa^2$ modulation is essential. The prototypical examples of biosensors in this class are those based on the periplasmic binding proteins (PBPs), which undergo a clamshell-type motion upon binding their target ligand.[33] Achieving substantial $\kappa^2$ modulation is quite challenging, but the effort is justified by the promise of eventually achieving broadly applicable designs for biosensors based on PBPs. This protein superfamily encompasses an exceptional diversity of ligand binding specificities and represents a rich source of binding modules for biosensor construction.[34] The considerations related to development and optimization of PBP-based biosensors are equally applicable to other biosensors based on conformational changes of single proteins.[10]

In the absence of extensive optimization, ratio changes for PBP-based biosensors tend to be quite modest. Some early examples include maltose biosensors with $\Delta R/R_{min} \approx 13\%$,[35] glucose biosensors with $\Delta R/R_{min} \approx 10\%$,[36] ribose biosensors with $\Delta R/R_{min} \approx 15-20\%$,[37] and glutamate biosensors with $\Delta R/R_{min} \approx 14\%$.[38] Ratio changes of this magnitude are attributable to small changes in distance and/or orientation and are consistent with a subtle conformational change of PBP. Fortunately, the empirical screening of libraries of linker variants have produced members of this class with dramatically improved $\Delta R/R_{min}$.

The strategy most often used for optimization of PBP-based biosensors is the systematic truncation of the two linkers that join the PBP to the donor and acceptor. For example, the $\Delta R/R_{min}$ for a glucose biosensor was improved from 9% to 39% by deletion of 15 and 16 residues from the N- and C-terminal linkers, respectively.[39] Likewise, deletion of ten residues from the N-terminal linker and three residues from the C-terminal linker improved the $\Delta R/R_{min}$ for a sucrose biosensor from 15% to 52%.[40] Although the exact mechanism has not been verified, it is likely that $\kappa^2$ modulation due to restricted FP conformational mobility is of greater importance than distance modulation.[39] This scenario is consistent with the observation that shorter linkers, which are expected to most severely limit conformational mobility, tend to result in the highest $\Delta R/R_{min}$. Indeed, the amount of linker deleted tends to be close to the maximum that can be deleted without adversely affecting protein folding and function. For example, in a recently reported effort to optimize the $\Delta R/R_{min}$ of a glutamate biosensor, the authors tested a library of variants that encompassed all possible combinations of N-terminal (0−15 residues) and C-terminal (0−10 residues) linker truncations.[41] Of the 176 constructs tested, one showed a substantial improvement ($\Delta R/R_{min} = 46\%$) over the original construct ($\Delta R/R_{min} = 18\%$). Furthermore, changing one linker by a single residue resulted in a biosensor with an unremarkable $\Delta R/R_{min}$, whereas decreasing the other linker by a single residue caused improper folding. This exquisite and unpredictable dependence on linker length is consistent with $\kappa^2$ modulation being the dominant mechanism for this type of biosensor.

Topological manipulation of FRET-based biosensors is another effective means of maximizing $\Delta R/R_{min}$. The linker modifications described above are not considered to be topological manipulation because the overall connectivity of the polypeptide chain does not change. The simplest topological change is to swap the position of the donor and acceptor.[42] However, this swap

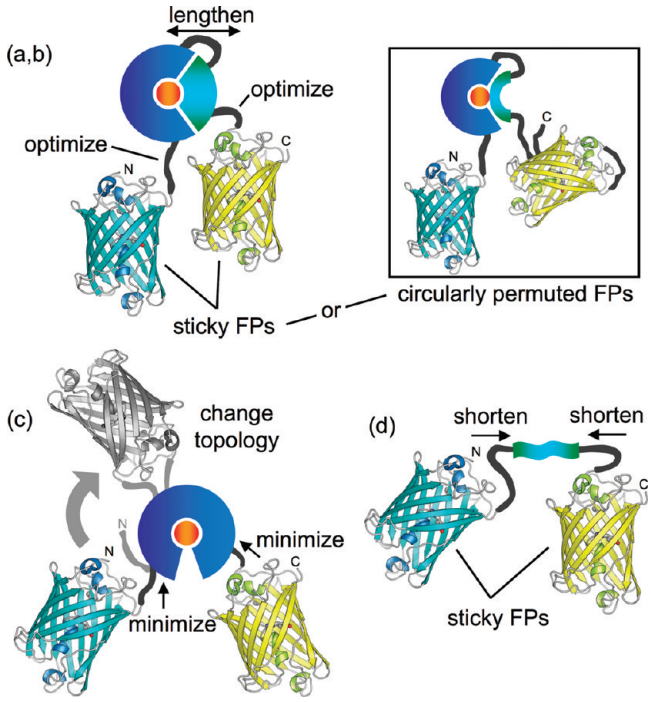


**Figure 5.** Strategies for optimization of FRET-based biosensors. (a−b) Optimization strategies for biosensors based on dramatic conformational changes (those shown in Figure 1a,b). (c) For biosensors based on relatively subtle conformational changes (those shown in Figure 1c), minimizing the conformational freedom of the FPs is the most effective optimization strategy. (d) For biosensors of the type shown in Figure 1d, it is desirable to bring the FPs as close together as possible without preventing access of the protease to the substrate.

is not expected to change $r$ or $\kappa^2$ (to a first approximation), and perhaps this explains why it is not commonly employed in biosensor optimization. A very effective topological change is to replace the donor and/or acceptor with circularly permuted variants.[18,19,43,44] For example, the $\Delta R/R_{min}$ of a $Ca^{2+}$ biosensor (Figure 1a) was improved from 100% to 560%,[18] and the $\Delta R/R_{min}$ of a cAMP-dependent protein kinase biosensor (Figure 1b) was improved from 18% to 35%[44] by systematically screening variants that incorporated circularly permuted FPs.

Topological manipulation of the conformationally dynamic domain is also an effective strategy for maximizing $\Delta R/R_{min}$. For example, the ratio changes observed at physiologically relevant concentrations of $Ca^{2+}$ were substantially improved by rearranging the domains of a $Ca^{2+}$ biosensor.[45] Insertion of at least one of the FPs into surface-exposed loops of the conformationally dynamic domain can also provide dramatic improvements in $\Delta R/R_{min}$. Moving the donor from an N-terminal fusion to an insertion in an internal loop improved the $\Delta R/R_{min}$ of a glutamate biosensor from 12% to 92%.[39] Because it is tethered through both termini, the internally fused FP is likely more conformationally restricted than the N-terminally fused, and thus $\kappa^2$ values further removed from 2/3 can be achieved. This strategy has been combined with linker manipulation to produce a glucose biosensor optimized for *in vivo* applications.[46]

## OUTLOOK AND CONCLUSION

During the next few years, we are sure to see the development of FPs with novel colors as well as the continual refinement and improvement of the existing color classes. Developments that would be particularly welcome in the area of FP-based biosensors include the engineering of FPs with improved photostability, increased brightness, monoexponential lifetime decays (for lifetime imaging), and narrower peak profiles. One highly anticipated development is a FP with absorbance and fluorescence in the NIR (650−900 nm); tissue is most transparent to light in this range.[47] Accompanying these developments in the properties of FPs, improved strategies for the optimization of biosensors will likely emerge. One exciting direction would be to use single cell analysis and sorting for rapid screening of very large libraries of biosensor variants. Most new approaches likely will focus on the streamlining of high-throughput empirical screens; it is difficult to envision computational or rational design strategies proving more effective in the near future.

This critical dissection of the relative importance of distance and orientation in the design of FRET-based biosensors has provided some clear guidelines that should assist any researcher in developing such a biosensor. It has also provided a realistic perspective on the gains that might be expected from a determined optimization effort. In terms of the initial design of a FRET-based biosensor, proteins that are designed to maximize $\Delta r$ are clearly preferred and represent the best possible starting point for further optimization. Starting with a design that relies primarily on $\kappa^2$ modulation means that further optimization will be more challenging and that achieving the minimally sufficient $\Delta R/R_{min}$ of 30% will be non-trivial. Figure 5 summarizes the optimization strategies that, based on literature precedent, are most likely to result in improved $\Delta R/R_{min}$ for the four basic classes of biosensors represented in Figure 1. These optimization strategies should not be taken as universally applicable rules that will benefit all biosensors. Rather, they should be viewed as guidelines for the construction of complete series of systematically modified variants that are then subjected to empirical screening. By following these rational guidelines, researchers will be efficiently investing their time and effort on those optimization strategies that are most likely to succeed.

## ACKNOWLEDGMENT

The author acknowledges the support of the Canada Research Chairs program, NSERC, and Alberta Ingenuity. He thanks Haley Carlson for assistance with the literature search and members of his group for proofreading of this manuscript.

*Robert E. Campbell is an associate professor and Canada Research Chair in Bioanalytical Chemistry in the Department of Chemistry of the University of Alberta. Research in his laboratory is focused on protein engineering and the development of new fluorescent protein variants for the construction of FRET-based biosensors. Address correspondence to him at the University of Alberta, Department of Chemistry, Edmonton, Alberta T6G 2G2, Canada (robert.e.campbell@ualberta.ca).*

## REFERENCES

(1) Lim, D. V.; et al. *Clin. Microbiol. Rev.* **2005**, *18*, 583–607.
(2) Miyawaki, A.; et al. *Nature* **1997**, *388*, 882–887.
(3) Chalfie, M.; et al. *Science* **1994**, *263*, 802–805.
(4) Campbell, R. E. *Scholarpedia* **2008**, *3*, 5410.
(5) Shaner, N. C.; Patterson, G. H.; Davidson, M. W. *J. Cell Sci.* **2007**, *120*, 4247–4260.
(6) Cubitt, A. B.; et al. *Trends Biochem. Sci.* **1995**, *20*, 448–455.
(7) Shimozono, S.; Miyawaki, A. *Methods Cell Biol.* **2008**, *85*, 381–393.
(8) Shaner, N. C.; Steinbach, P. A.; Tsien, R. Y. *Nat. Methods* **2005**, *2*, 905–909.

(9) Kogure, T.; et al. *Nat. Biotechnol.* **2006**, *24*, 577–581.
(10) VanEngelenburg, S. B.; Palmer, A. E. *Curr. Opin. Chem. Biol.* **2008**, *12*, 60–65.
(11) Baird, G. S.; Zacharias, D. A.; Tsien, R. Y. *Proc. Natl. Acad. Sci. U.S.A.* **1999**, *96*, 11,241–11,246.
(12) Nagai, T.; et al. *Proc. Natl. Acad. Sci. U.S.A.* **2001**, *98*, 3197–3202.
(13) Forster, T. *Naturwissenschaften* **1946**, *33*, 166–175.
(14) Forster, T. *Discuss. Faraday Soc.* **1959**, *27*, 7–17.
(15) Wallrabe, H.; Periasamy, A. *Curr. Opin. Biotechnol.* **2005**, *16*, 19–27.
(16) dos Remedios, C. G.; Moens, P. D. *J. Struct. Biol.* **1995**, *115*, 175–185.
(17) Miyawaki, A.; Tsien, R. Y. *Methods Enzymol.* **2000**, *327*, 472–500.
(18) Nagai, T. *Proc. Natl. Acad. Sci. U.S.A.* **2004**, *101*, 10,554–10,559.
(19) Palmer, A. E.; et al. *Chem. Biol.* **2006**, *13*, 521–530.
(20) Borst, J. W.; et al. *Biophys. J.* **2008**, *95*, 5399–5411.
(21) Pham, E.; et al. *Structure* **2007**, *15*, 515–523.
(22) Kimura, R. H.; Steenblock, E. R.; Camarero, J. A. *Anal. Biochem.* **2007**, *369*, 60–70.
(23) Evers, T. H.; et al. *Protein Eng. Des. Sel.* **2008**, *21*, 529–536.
(24) van Dongen, E. M.; et al. *J. Am. Chem. Soc.* **2007**, *129*, 3494–3495.
(25) Nguyen, A. W.; Daugherty, P. S. *Nat. Biotechnol.* **2005**, *23*, 355–360.
(26) Vinkenborg, J. L.; et al. *ChemBioChem* **2007**, *8*, 1119–1121.
(27) Ohashi, T.; et al. *Protein Sci.* **2007**, *16*, 1429–1438.
(28) Ouyang, M.; et al. *Proc. Natl. Acad. Sci. U.S.A.* **2008**, *105*, 14,353–14,358.
(29) Fuller, B. G.; et al. *Nature* **2008**, *453*, 1132–1136.
(30) Evers, T. H.; et al. *J. Mol. Biol.* **2007**, *374*, 411–425.
(31) Zacharias, D. A.; et al. *Science* **2002**, *296*, 913–916.
(32) Jost, C. A.; et al. *ChemBioChem* **2008**, *9*, 1379–1384.
(33) Lalonde, S.; Ehrhardt, D. W.; Frommer, W. B. *Curr. Opin. Plant Biol.* **2005**, *8*, 574–581.
(34) Dwyer, M. A.; Hellinga, H. W. *Curr. Opin. Struct. Biol.* **2004**, *14*, 495–504.
(35) Fehr, M.; Frommer, W. B.; Lalonde, S. *Proc. Natl. Acad. Sci. U.S.A.* **2002**, *99*, 9846–9851.
(36) Fehr, M.; et al. *J. Biol. Chem.* **2003**, *278*, 19,127–19,133.
(37) Lager, I.; et al. *FEBS Lett.* **2003**, *553*, 85–89.
(38) Okumoto, S.; et al. *Proc. Natl. Acad. Sci. U.S.A.* **2005**, *102*, 8740–8745.
(39) Deuschle, K.; et al. *Protein Sci.* **2005**, *14*, 2304–2314.
(40) Lager, I.; et al. *J. Biol. Chem.* **2006**, *281*, 30,875–30,883.
(41) Hires, S. A.; Zhu, Y.; Tsien, R. Y. *Proc. Natl. Acad. Sci. U.S.A.* **2008**, *105*, 4411–4416.
(42) Kwok, S.; et al. *Biochem. Biophys. Res. Commun.* **2008**, *369*, 519–525.
(43) Mank, M.; et al. *Biophys. J.* **2006**, *90*, 1790–1796.
(44) Allen, M. D.; Zhang, J. *Biochem. Biophys. Res. Commun.* **2006**, *348*, 716–721.
(45) Mank, M.; et al. *Nat. Methods* **2008**, *5*, 805–811.
(46) Takanaga, H.; Chaudhuri, B.; Frommer, W. B. *Biochim. Biophys. Acta, Biomembr.* **2007**, *1778*, 1091–1099.
(47) Weissleder, R. *Nat. Biotechnol.* **2001**, *19*, 316–317.
(48) Zhang, J. *Proc. Natl. Acad. Sci. U.S.A.* **2001**, *98*, 14,997–15,002.
(49) Ting, A. Y.; et al. *Proc. Natl. Acad. Sci. U.S.A* **2001**, *98*, 15,003–15,008.
(50) Heim, R.; Tsien, R. Y. *Curr. Biol.* **1996**, *6*, 178–182.
(51) Ai, H.; et al. *Biochem. J.* **2006**, *400*, 531–540.
(52) Day, R. N.; Booker, C. F.; Periasamy, A. *J. Biomed. Opt.* **2008**, *13*, 031203.

AC802613W